

Received November 10, 2014, accepted March 24, 2015, date of current version April 22, 2015.

Digital Object Identifier 10.1109/ACCESS.2015.2422842

# Silicon Nanowire Field-Effect Transistors— A Versatile Class of Potentiometric Nanobiosensors

LUYE MU<sup>1,2</sup>, YE CHANG<sup>1</sup>, SONYA D. SAWTELLE<sup>3</sup>, MATHIAS WIPF<sup>2</sup>, XUOXIN DUAN<sup>1</sup>,  
AND MARK A. REED<sup>2</sup>, (Senior Member, IEEE)

<sup>1</sup>State Key Laboratory of Precision Measuring Technology and Instruments, Tianjin University, Tianjin 300072, China

<sup>2</sup>Department of Electrical Engineering, Yale University, New Haven, CT 06520, USA

<sup>3</sup>Department of Applied Physics, Yale University, New Haven, CT 06520, USA

Corresponding author: X. Duan (xduan@tju.edu.cn)

This work was supported in part by the Tianjin Applied Basic Research and Advanced Technology under Grant 14JCYBJC41500 and in part by the 111 Project under Grant B07014. The work of L. Mu was supported by the Natural Sciences and Engineering Council of Canada. The work of M. A. Reed was supported in part by the Research Project under Grant FA8650-9-D-5037 0019 and in part by the U.S. Army Research Office under Grant MURI W911NF-11-1-0024.

**ABSTRACT** Silicon nanowire field-effect transistors (Si-NW FETs) have been demonstrated as a versatile class of potentiometric nanobiosensors for real time, label-free, and highly sensitive detection of a wide range of biomolecules. In this review, we summarize the principles of such devices and recent developments in device fabrication, fluid integration, surface functionalization, and biosensing applications. The main focus of this review is on CMOS compatible Si-NW FET nanobiosensors.

**INDEX TERMS** Biosensors, field effect transistors, nanowires, semiconductor nanostructures, nanobiosensors.

## I. INTRODUCTION

The role of biosensing in society has gained increasing importance over the last several decades, reflected in the rapid growth of the global market. According to *Global Industry Analysts, Inc.*, the global market for biosensor devices is expected to reach \$20 billion by the year 2020. Sensitive detection and quantification of bio-analytes is a driving force for innovation in many vital fields such as biomedical research, clinical medicine, agriculture, food safety, environmental monitoring and homeland security. Across these diverse applications of biosensors, there is a common demand for properties such as high sensitivity, low detection limit, large dynamic range, rapid and real-time detection, low cost and miniaturization. Modern advancements in nanomaterials and nano-scale fabrication have enabled a new generation of biosensors that can more easily satisfy these needs through improved performance, smaller size, and novel functionality. These nanobiosensors are sub-micrometer sized in at least one dimension, which allows them to possess very large surface area to volume ratios. In many cases their small footprint makes them well suited for high-density sensor arrays, lab-on-chip systems, and single-cell interfacing.

Classification schemes for biosensors traditionally focus on either the biological element e.g. antibody, enzyme,

or nucleic acid, or on the transducing element e.g. potentiometric, amperometric, or fluorometric transduction [1]. Although the operation of the biological element can vary, all potentiometric biosensors utilize a transduction element that operates under a change in electrical potential between a reference electrode and a working surface. This category encompasses all varieties of ion-selective electrodes (ISEs) and ion-sensitive field effect transistors (ISFETs). An ISE is a two-terminal system wherein the voltage between the membrane-enclosed indicator and reference electrode is modulated by the activity of ions with respect to the selective membrane. In contrast, ISFETs employ a three-terminal configuration with an active channel whose current is modulated in the presence of charged species. The advantage of an ISFET over an ISE is that an FET has intrinsic amplification. We also note here that the requirement of electrical charge for potentiometric transduction does not significantly restrict applications in that most biomacromolecules and cells acquire a net charge in solution at physiological pH. Clever modifications can also enable sensing of neutral molecules on some of these platforms [2]–[4].

Nanobiosensors falling under the ISFET umbrella include quasi-1D FETs utilizing top-down and bottom-up semiconducting wires, conducting polymer wires or carbon

nanotubes (CNTs) and 2D FETs which utilize naturally 2D materials. The 1D FETs are claimed to benefit from an extreme surface area to volume ratio which permits effective channel gating from even just a few adsorbed analyte molecules. Cui et al. were the first to execute this geometry: In 2001 they used vapor-liquid-solid (VLS) grown silicon nanowires (Si-NWs) for pH sensing and detected the binding of streptavidin protein on biotin-labeled wires [5]. Such “bottom-up” style FETs have since been used for the full spectrum of biosensing applications (i.e. detection of DNA, antibodies, enzymes, cells, aptamers, bioelectricity, etc.) with charged based or electrochemical sensing [6]–[8]. Relatively soon after, the top-down fabricated nanowire FET was introduced as a sensing platform [9]–[11] in order to address the problems of placement, integration, and reproducibility encountered with bottom-up materials. Such concerns apply equally to the CNT 1D FETs, in addition to the challenge of chiral vector selection, but nonetheless they have been demonstrated in a wide variety of biosensing niches [12]–[17]. Most recently, 1D FETs using polymeric nanowires have been developed, which enjoy cheaper fabrication and more customizable functionalization than semiconductor wires, but exhibit inferior electrical properties [18]–[21].

The 2D graphene-based FETs exhibit an enhanced surface sensitivity like the 1D FETs, as well as possess a minimal band-gap and high in-plane carrier mobility derived from the confinement of the carbon lattice [22]. These devices have been utilized for pH sensing [23], [24], as a possible reference electrode [25], as well as specific protein [26], [27] and DNA [28]–[30] sensing. Using graphene FETs, Huang et al. have demonstrated redox-based glucose detection with an enzyme-functionalized surface [31] and Cohen-Karni et al. have provided a dramatic demonstration of cell-interfacing by monitoring the electrical activity of embryonic heart cells [32]. Recently 2D FETs using a single monolayer sheet of molybdenum disulfide (MoS<sub>2</sub>) as the active channel have been employed for pH sensing and aqueous label-free protein detection in the femtomolar range [33].

Within the ISE class of potentiometric sensors, nanotechnology has led to rationally designed solid state membrane nanopores [34], [35], and improved solid-contact electrode materials such as CNTs [36], [37] and gold nanoparticles [38]. These refinements to the conventional ISEs notwithstanding, we choose to focus this review on the ISFET class where nanotechnology has had a more transformative impact, and in particular the silicon nanowire variety due to manufacturability. We provide first a brief overview of the general FET sensing structure, and then the particulars of Si-NW FET fabrication. A short discussion of fluidic integration, multiplexing, functionalization, and performance limitations is followed by a survey of the various biological applications that have been successfully addressed by Si-NW FETs. A discussion of Si-NW FETs compared to other biosensing platforms can be found elsewhere [39].

## II. DEVICE FABRICATION AND INTEGRATION

### A. DEVICE STRUCTURE AND FABRICATION

Over the years, many variations of FET-based potentiometric sensors have been developed. They share many (but not all) common features with the conventional MOSFET. FET-based devices are three-terminal structures with a gate, drain, and source. The conductance of the channel between the source and drain is modulated by the voltage at the gate terminal. In MOSFETs, the metallic gate is in direct contact with the dielectric over the channel, but in biological FET (bioFET) sensors, the gate (reference) electrode is a distance away from the dielectric, with an intervening sample fluid. Changes at the dielectric-solution interface alter the surface potential, which acts as an additional gate voltage. A gate voltage ( $V_{GS}$ ) is applied using a reference electrode to set the operating point of the device, and the conductance of the channel is measured by applying a drain (D) to source (S) voltage ( $V_{DS}$ ). P-type devices display a decrease in conductance with the binding of positive charges to the surface, and n-type devices display an increase (Figure 1).

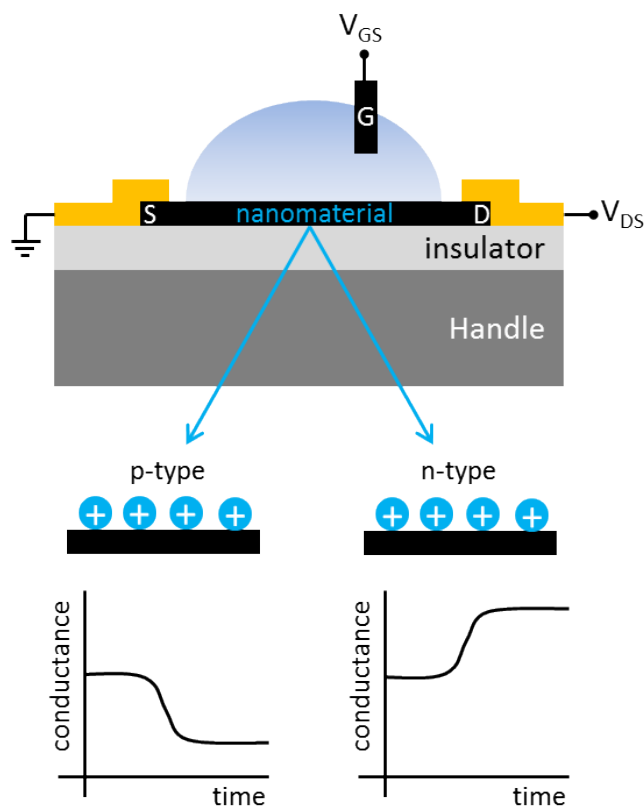


FIGURE 1. Operation schematic of a nano BioFET.

The expression for the linear regime operation of MOSFETs applies to bioFETs, with drain current ( $I_{DS}$ ) described as:

$$I_{DS} = \mu C_{ox} \frac{W}{L} \left[ (V_{GS} - V_T) V_{DS} - \frac{1}{2} V_{DS}^2 \right] \quad (1)$$

where  $\mu$  is the channel mobility,  $C_{ox}$  is the dielectric capacitance,  $W$  and  $L$  are width and length dimensions

of the device, and  $V_T$  is the threshold voltage of the device. When the device is exposed to solution, a surface potential ( $\psi$ ) develops at the dielectric-solution interface, which is a function of surface and solution characteristics. Thus, the  $V_T$  in (1) can be expressed as:

$$V_T = E_{ref} - \psi + \chi^{sol} - \frac{\Phi_{Si}}{q} - \frac{Q_t}{C_{ox}} + 2\phi_f \quad (2)$$

where  $E_{ref}$  is the reference electrode potential,  $\chi^{sol}$  is the surface dipole potential of the solvent,  $\Phi_{Si}$  is the channel work function,  $q$  is elementary charge,  $Q_t$  is a combination of depletion charges in the semiconductor, accumulated charges in the dielectric, and interface trap charges, and  $\phi_f$  is the Fermi potential. In the case where gate and drain voltages are fixed, the only variable term in the equation is  $\psi$ , which is a function of physical and chemical changes at the surface of the oxide. Thus, monitoring changes via the change in  $V_T$  is an effective way of sensing changes at the dielectric-electrolyte interface.

Over time, variations on the bioFET has been developed to allow for the detection of many analytes, these variations, such as enzyme-FETs, chemical-FETs, etc., are realized by functionalizing different specific receptors at the dielectric-solution interface. The difference between different types of nano FET-based sensors lies mainly with the interface and channel material. Out of all the bioFETs that have been studied, micro- and nanofabricated silicon has been the most popular material for the channel.

Approaches to fabricating Si-NW for sensors have been categorized into two main groups: bottom up and top down assembly. The first Si-NW FETs were grown by bottom up VLS techniques [5], [40], then harvested and deposited on a substrate. The contacts were subsequently patterned by lithography. VLS synthesis techniques nominally use metal nanoparticles to catalyze nanowire formation and define nanowire size. High quality nanowires with low defect densities and smooth sidewalls can be fabricated this way, however this technique is not conducive to scaling for mass production. Various approaches have been proposed to aid the arrangement of 1D nanomaterials on a substrate, including many fluidic assisted [41]–[45] and electrically controlled [46]–[48] methods. Nevertheless, the yield and repeatability was still not optimal. This led to an increase in the use of top down device fabrication technologies, which allowed nanowire dimensions and locations to be precisely defined on the wafer. Top-down fabricated nanowires are typically defined on ultrathin silicon on insulator (UTSOI) wafers using electron beam lithography (EBL), with the contacts and metallization defined using optical lithography [10], [49], [50]. In order to further reduce dimensions, a subsequent wet chemical etch [11], [51]–[53], electrochemical etch [54], or oxidation [55], [56] is often used. Unfortunately, EBL is an expensive and time-consuming process, and is not amenable to large-scale manufacturing. Therefore several groups have innovated some creative process flows for fabricating nanowires based

on the anisotropy of silicon and plane-dependent wet etching, without needing EBL. For example, Chen et al. used a  $\text{Si}_3\text{N}_4$  etch mask patterned by conventional lithography to generate nanoribbons, followed by anisotropic wet etching and thermal oxidation to define two triangular cross-section nanowires from the edges of each nanoribbon [57]. Stern et al. also used a mask-and-etch method to fabricate nanowires from optically defined nanoribbons, using tetramethylammonium hydroxide (TMAH) [11]. Another advantage of using a highly anisotropic etching method instead of oxidation is that it also provides refinement of nanowire edges. For instance, in addition to thinning the nanowires, TMAH also provided a smoothing effect for sidewall imperfections not aligned to the exposed [111] plane, creating sensitive structures with extremely low noise [58]. Recently, many groups have opted to use larger width devices such as nanoribbons and nanoplates, with much more relaxed fabrication requirements [59]–[61].

Although single-crystalline silicon nanowires have great signal to noise ratios, their fabrication incurs significant costs due to the need for UTSOI wafers as starting materials. Therefore, polysilicon nanowires have been explored as a cheaper alternative. Amorphous silicon of approximately 100 nm thickness can be deposited on oxide substrates by low pressure chemical vapor deposition (LPCVD), annealed to form grains, then subsequently etched to form wires [62]. Just like with single-crystalline nanowires, various masking, trimming and spacer techniques have been used to define sub-micron dimension wires in polysilicon [62]–[64]. However, one would expect the intrinsic noise of polycrystalline nanowires to be inferior compared to single crystalline nanowires due to the increased grain-boundaries and interface traps. A way to fabricate single crystalline Si-NW FET biosensors without needing to use UTSOI is to create fin-like structures from bulk silicon (ie. FinFETs). Rigante et al. showed fully-depleted bio-FinFETs with critical dimensions of  $\sim 20$  nm with excellent electrical properties [65].

In the context of modern integrated circuit technology, there is significant value in making the device fabrication CMOS-compatible. Many groups have developed CMOS-compatible process flows [11], [51], [61], [64]–[66], and some have successfully integrated on-chip memory components with the sensors [67]. Huang et al. used the 0.35  $\mu\text{m}$  2P4M standard CMOS process to fabricate a polysilicon NW based biosensor system-on-a-chip complete with an amplifier, an analog to digital converter, a microcontroller, and a wireless transceiver [68]. With the advantages of scalability and potential integration with on-chip addressing and signal processing components, CMOS compatible Si-NW FETs can meet the current demand for a sensitive, high-throughput and multiplexed biosensor. Similar device characteristics allow the use of a global gating scheme in multiplexing, and various calibration methods can be used to account for the small device-to-device variations and drift [69].

The dielectric coating over the channel is one of the key components dictating the performance of the Si-NW device. Traditionally, SiO<sub>2</sub> is used due to the ease of fabrication via oxidation. However, SiO<sub>2</sub> is semipermeable to small positive ions such as K<sup>+</sup> and Na<sup>+</sup>, thus significantly limiting device stability and lifetime when operating in high ionic strength solutions. High *k* dielectrics such as Si<sub>3</sub>N<sub>4</sub>, Al<sub>2</sub>O<sub>3</sub>, and HfO<sub>2</sub>, are known to improve device leakage, stability, and hysteresis due to the high quality and density of films [70], [71]. In addition, many of them exhibit near-Nernstian responses to pH [59], [72]–[74]. The most popular method for depositing good quality high *k* dielectrics is by atomic layer deposition (ALD), a self-limiting process capable of creating uniform, dense, conformal, and pin-hole free layers. Nevertheless, since high *k* dielectrics are deposited rather than grown, the interface between the channel and the dielectric is rarely good enough quality to match that of Si-SiO<sub>2</sub>, thereby increasing interface traps and device noise. Therefore, the correct dielectric to use for a sensor is highly dependent on the application – SiO<sub>2</sub> covered devices may have better signal to noise ratios for short term operations for detecting biomolecules, whereas high *k* covered devices may have better signal to noise ratios for long term operations or pH-based measurements. Some groups have investigated multi-layer dielectric stacks to simultaneously take advantage of the excellent Si-SiO<sub>2</sub> interface and high *k* layer qualities [71].

For the remainder of this review, we focus mainly on sensing examples from top-down fabricated silicon nanowires. However, since most biomolecular detection schemes can be generally applied to all FET-type sensors regardless of fabrication method or device material, we have also included a few notable examples of works from bottom up nanowires and nanowires made from other channel materials.

## B. FLUIDIC INTEGRATION

Sample scarcity is often an issue for biological samples – in particular physiological samples. Therefore, being able to limit the required sample amount for analysis is advantageous. BioFETs can be made into planar, high-density arrays, which are conducive to microfluidic integration. Two types of microfluidic setups are commonly used for sample delivery: reservoirs and microchannels. The fluid cells are typically made from polydimethylsiloxane (PDMS) due to its excellent optical transparency and biocompatibility.

Reservoirs over FET devices are typically designed to hold a few to hundreds of microliters of sample, and sample exchange is done manually through pipetting [11], [75]. Drawbacks of the microwell method include evaporation of sample, which precludes long term measurements from being conducted on small samples, and difficulty in conducting kinetic measurements due to the consumption of analytes.

Microchannels have micrometer dimensions, but require more reagent overall due to the need for continuous flow. Flow-based delivery allows greater potential for system automation, with accurate sample volume dispensing

and automatic sample switching [76]. However, flow in microfluidic channels can be laminar, which can restrict the interaction between the injected molecules and the sensor surface [77]. It was also shown that variation in flow speed induces a change in conductance in the underlying FET [76], [78]. However, many groups used constant speed flow to deliver solutions, and were able to obtain consistent results at low sample concentrations [76], [79]–[81].

The integration of a reference electrode is an essential yet nontrivial component of fluidic integration for Si-NW FETs. In open reservoir sensing, the solution gate electrode can be inserted directly into the open reservoir. However, in flow experiments, the reference electrode is either integrated into the inlet/outlet tubing [82]–[84], or fabricated on-chip. Although on-chip Ag/AgCl reference electrodes have been reported [85], the use of any metal (typically gold or platinum) with a differential setup may offer a more robust technique due to the ability to decouple other environmental factors [76]. The ability to create an effective differential system is directly dependent on the ability to control surface functionalization across an array of devices.

## C. FUNCTIONALIZATION

In order to detect specific biomolecular interactions, nanowire devices need to be functionalized with bio-receptors. The choice of functionalization scheme and specifics of the procedure affect the quality of the bio-receptor layer e.g. density, thickness and orientation. In turn, this layer strongly impacts performance metrics of the sensor such as sensitivity, stability, reproducibility and regenerative capacity [86], [87]. Different strategies have been applied for Si-NW surface functionalization [88]. For silicon oxide surfaces, covalent modification through silane chemistry has been the most common technique (Figure 2A). A typical silane agent is 3-aminopropyltriethoxysilane (APTES). APTES introduces a primary amine terminal group, which can further react with aldehyde, carboxylic acid and epoxy groups present on proteins and other biomolecules. Dorvel et al. compared the effect of different linker chemistries on protein sensing performance [89]. Additionally, 3-mercaptopropyl-trimethoxysilane (MPTMS), (3-Glycidoxypropyl)-methyl-diethoxysilane (GPTS) and (3-bromopropyl)trichlorosilane have been reported to introduce thiol [90], epoxy [91] and bromide [92] terminal group, respectively. Alternatively, for hydrogen-terminated Si-NWs (oxide free nanowires), alkenes (or alkynes) can be used to form a true organic monolayer with higher chemical stability compared with silane chemistry alkenes (Figure 2B) [86]. In addition to covalent attachments, some non-covalent approaches are also noteworthy. For instance,  $\beta$ -cyclodextrin ( $\beta$ -CD) based supramolecular layers have been used as linkers for Si-NWs (Figure 2C) [93]. Owing to the reversible host-guest chemistry of  $\beta$ -CD, the sensor surface can be fully regenerated. Regeneration of the sensor surface would be highly beneficial for their use, since it

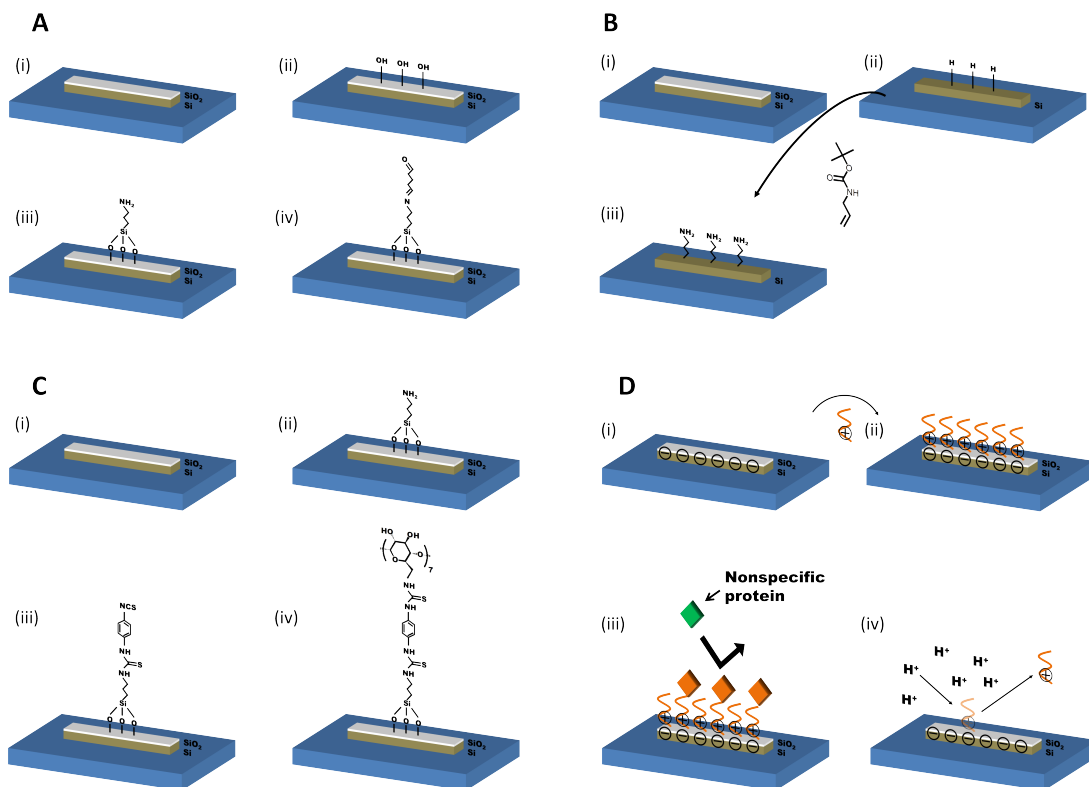


**FIGURE 2.** Si-NW functionalization schemes. (A) Silane chemistry (APTES) on Si-NW: (i) pristine Si-NW, (ii) hydroxylation of silicon oxide surface, (iii) silanization, (iv) further reaction with aldehyde. (B) Alkene modification of hydrogen-terminated Si-NW: (i) pristine Si-NW, (ii) BOE etching of silicon oxide surface, (iii) functionalization of hydrogen terminated SiNW with tert-Butyl allylcarbamate. (C) Functionalization of Si-NW with  $\beta$ -CD supramolecular layer: (i) pristine Si-NW, (ii) silanization of Si-NW with APTES, (iii) further reaction with p-phenylenediisothiocyanate and (iv) amino-functionalized  $\beta$ -CD. (D) Functionalization of Si-NW with biocompatible polyelectrolytes: (i) pristine Si-NW, (ii) the positively charged copolymers are attached to the sensor surface by electrostatic forces, (iii) protein non-specific binding is blocked by the polyelectrolyte thin film, (iv) sensor regeneration by recharging the oxide surface with low pH solutions.

provides the possibility to measure analytes using the same high quality device and avoids the variations in device characteristics from one sensor to another. In a more recent work, Duan et al. demonstrated a simpler way to regenerate the sensor surface [94]. Devices were coated with biocompatible polyelectrolyte thin films consisting of poly-*L*-Lysine backbones grafted with oligo-ethylene-glycol (OEG) (Figure 2D). The mono-layer films are attached to the sensor surface by electrostatic forces between the negatively charged surface of the oxide and the positively charged copolymers. The sensor regeneration is achieved by simple pH treatment, relying on separation of the film at low pH solutions due to positive charging of the oxide surface. Moreover, the incorporated OEG groups demonstrate resistance to protein non-specific binding.

The small size, reproducibility, and ease of electronic integration make CMOS-compatible Si-NW FETs amenable to systems requiring large arrays of multiply-functionalized sensors. Such an approach can improve signal reliability by providing many independent sensing responses [77], [95], and by enabling differential measurements where drift and environmentally induced noise are monitored on nearby reference devices [50], [84]. However, the primary challenge

in multiplexing Si-NW FETs is differential functionalization individual devices. Commercially available fluid spotting systems [96], [97] are commonly used, and microfluidics can allow selective fluidic addressing of devices, but these approaches preclude very dense spacing. Park et al. cleverly exploited the joule heating of a driven nanowire for selective ablation of a blocking polymer layer and thus selective exposure to functionalizing molecules (Figure 3A) [98]. Stern et al. used electrodeposition to differentially functionalize ITO electrodes with derivatized phenols by a process compatible with conducting and semi-conducting substrates (Figure 3B) [99]. Similarly Bunimovich et al. used a functionalization precursor layer which is activated by the electric field around an individual biased Si-NW [100]. Dip-pen nanolithography is another promising approach that has been demonstrated on bare  $\text{SiO}_2$  to create a spot array with 350 nm spacing (Figure 3C) [101].

Once the challenge of differential surface functionalization is overcome, higher density Si-NW arrays can be used to quantify large panels of different analytes simultaneously. Small scale diagnostic panel-style systems have already been shown for cardiac health markers [97], [102], cancer markers [96], [103] and viral DNA [104]. Electronic nose

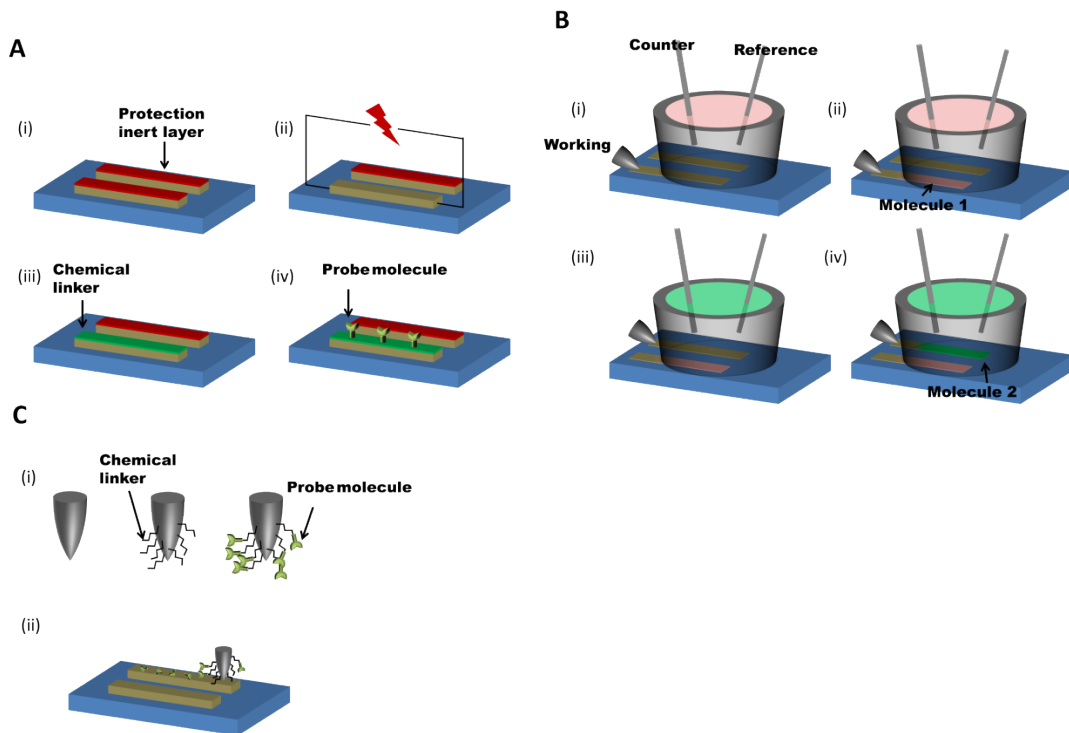


**FIGURE 3.** Process schematics for selective and multiplexed functionalization of Si-NWs. (A) Functionalization by Joule heating: (i) the deposition of protection inert layer, (ii) Joule heating and the ablation of the protective layer, (iii) surface functionalization with chemical linker and (iv) probe molecule. (B) Functionalization by surface electrochemical polymerization: (i) the three-electrode electrochemical cell (working electrode is contacted by a microprobe), (ii) molecule 1 is selectively functionalized by electrochemical polymerization, (iii) and (iv) the second nanowire is subsequently functionalized with molecule 2. (C) Functionalization by dip-pen nanolithography: (i) the modification of an AFM tip with chemical linker and thus probe molecule is easily adsorbed, (ii) the dip-pen nanolithography process, and probe molecule is thus transported to the surface.

systems based on pattern recognition of differential response across many differently functionalized wires have also been implemented [105]–[107].

### III. PERFORMANCE LIMITATIONS OF NANOWIRE SENSORS

Over the years, the field of “nanowire sensors” has also evolved to include nanoribbon and nanoplate sensors. A large body of literature is available to highlight all the applications that have been demonstrated using devices with a large range of dimensions, however, many of these works are presented without background information regarding why a device of that particular size was chosen. Therefore, before discussing applications, an important issue is device scaling – i.e., what is the optimal size of the nanosensor device which will enable the best performance?

The tremendous research interest in the nanowire field has been based on the premise that nanowire devices offer excellent current sensitivity due to their large surface area-to-volume ratio, as demonstrated by the metric of *sensitivity* ( $S$ ) =  $\frac{\Delta I}{I}$ , with  $\Delta I$  being the change in current upon binding or unbinding of the target molecule at the surface, and  $I$  being the original current level. With this being the metric, smaller devices are clearly superior,

and significant research effort was devoted to scaling to small dimensions, approaching 1D. In addition, a few other advantages of downscaling dimension have come to light – in addition to a small improvement in the electrostatics, the geometry of thinner wires may also offer reduced detection time due to an improvement in the analyte diffusion kinetics [108]. However, when trying to measure low concentration samples, the limit of detection of the devices is the critical parameter, and the metric of sensitivity provided above offers no information in this regard. The characteristic that determines the smallest resolvable  $\Delta I$  is the intrinsic current noise ( $\delta i$ ) of the sensor. Therefore the metric of signal to noise ratio (SNR) becomes more relevant in comparing the detection limit of the sensors, with higher SNR corresponding to lower detection limits [109].

When using SNR as the metric of interest, one can see that smaller devices may not be better for every application. The SNR of a measurement can be described as [109]:

$$SNR = \frac{\Delta I}{\delta i} = \frac{g_m \times \Delta \psi}{\sqrt{\ln\left(\frac{f_2}{f_1}\right)} \times \sqrt{S_I(f)}} \quad (3)$$

where  $g_m$  is the transconductance,  $\Delta \psi$  is the change in surface potential,  $f_2$  and  $f_1$  are the largest and smallest

frequencies sampled in the measurement, and  $S_I(f)$  is the drain current noise power density at a certain frequency  $f$ . We can expand (3) further by considering the number fluctuation model [110], [111]:

$$\Delta\psi = \frac{\Delta Q}{A \times (C_{ox} + C_{dl})} \quad (4)$$

and

$$S_I = g_m^2 \times S_{VFB} = g_m^2 \times \frac{\lambda k T q^2 N_{ot}}{A C_{ox}^2 f} \quad (5)$$

where  $\Delta Q$  is the total change in bound surface charge,  $A$  is the device surface area,  $C_{dl}$  is the double layer capacitance per unit area,  $S_{VFB}$  is the noise in the flatband voltage,  $\lambda$  is the characteristic tunneling distance,  $k$  is the Boltzmann constant,  $T$  is temperature, and  $N_{ot}$  is the interface trap density. Thus we can see that SNR can be represented in the following form:

$$SNR \propto \frac{\text{constant} \times \Delta Q}{\sqrt{A}} \quad (6)$$

From (6) one can see that if  $\Delta Q$  scales with area, SNR is higher for devices with larger surface area; conversely, if  $\Delta Q$  is constant, SNR is higher for devices with smaller area. For common diagnostic applications for concentration determination, the probability of analyte binding scales linearly with available surface area, therefore nanoribbons and nanoplates may be more desirable. Indeed, noise studies of pH measurement performance from several groups have recently demonstrated the advantage of larger area devices in this aspect [112], [113]. On the other hand, in the case of single-molecule kinetic studies, where only one single receptor is engineered on each device such that only one analyte is allowed to bind at any time, smaller nanowire devices may be more desirable. Of course, these conclusions assume constant interface trap density for the comparative devices (however, different sized devices often require different fabrication techniques, which can significantly alter the noise level). Moreover, the calculations do not take into account any quantum confinement induced volume inversion effects, which may play into effect at very small wire widths of 5-10 nm to decrease device noise [111].

From a device perspective, the detection limit is determined by the device noise. However, the detection limit of the entire system is also dependent on its biochemical characteristics, including the rate of analyte diffusion to the surface, and the affinity of the analyte-receptor interaction. These factors together set the lower bound on the dynamic range of the nanosensor, defined as the range of analyte concentration over which the concentration can be extracted from the device response.

In order for the sensor to be robust in many real world applications, an equally as important characteristic is the upper limit of the dynamic range. For pH detection, a large dynamic range is not a problem, as a pH difference of 14 units would result in a maximum surface potential

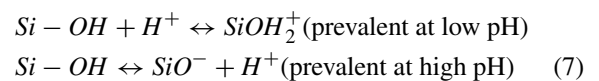
change of  $\sim 0.84V$ . This threshold shift can be easily designed to lie within the linear regime of the FET. For charged molecule sensing, many factors limit the upper bound of the dynamic range. A significant advantage of real time methods such as nanoFETs is that *two* pieces of information are available: the total value of the signal change at equilibrium, and the rate of the signal change. Therefore, even within the concentration range where the surface receptors would saturate at equilibrium, the kinetics of the initial binding can still be used to distinguish between concentrations, allowing one to effectively extend the dynamic range compared to an end-point measurement [82]. Therefore, the upper bound of the dynamic range is limited by the temporal resolution of the measurement before the surface receptors are saturated. FETs have the ability to sample at very fast rates due to their small RC time constants, potentially allowing observation of kinetics in the high concentration regime, since molecular binding kinetics are significantly slower in comparison. It is important to note that the intrinsic gain of an FET enables simple, sensitive, and fast measurements, eliminating the need for more complex measurement approaches (e.g. lock-in detection), and thus enabling higher speed for maximum dynamic range when necessary.

For most applications, there is a biochemically or clinically meaningful concentration range for the target analyte. For instance, for the cardiovascular disease marker cardiac troponin I, the range is from the normal serum level ( $<0.01$  ng/mL) to the peak level during myocardial infarction (50-100 ng/mL) [114]. An ideal sensor would have a dynamic range that encompasses the target relevant range.

## IV. BIOSENSING APPLICATIONS

### A. pH SENSING

In many biological processes, minute pH changes happen as a result of proton release or uptake by the biochemical reactions involved [75]. Therefore, determination of pH is a prerequisite for the monitoring of many biochemical processes. The mechanism of pH sensing with a FET is based on the amphoteric nature of the terminal groups at the solution-dielectric interface, which allows the surface charge state to change as it protonates or deprotonates [115]. The process is described by (7) for SiO<sub>2</sub> surfaces, where protonation and deprotonation of surface hydroxyl groups determine the surface charge:



Compared with the traditional ISFET, Si-NWs offer the advantages of smaller size and easy integration into cells or other living systems without influencing the behavior of the biological system (however, other than this aspect there is no apparent advantage of aggressive device scaling for pH sensing). After the first demonstration of pH sensing on CMOS-compatible, APTES functionalized

Si-NWs in 2007 [11], different approaches have been investigated to improve various aspects of pH sensing, including sensitivity, linearity, dynamic range and stability. Sensitivities ranging from 30 mV/pH to 60 mV/pH (Table 1) have been observed experimentally [49], [59], [61], [67], [72], [74], [76], [83], [115]–[119], with high-k dielectric materials coatings, (e.g. Al<sub>2</sub>O<sub>3</sub> [59] and HfO<sub>2</sub> [74]) occupying the higher end of the sensitivity spectrum. We note that although not all references in Table 1 use fully-CMOS-compatible processes, the aforementioned improvements made to pH sensing use CMOS-compatible techniques. The intrinsic sensitivity of the dielectric surface cannot exceed 59.2 mV/pH at 25 °C, as dictated by the Nernst Limit. For instance, Dorvel et al. achieved a 55.8 mV/pH sensitivity and excellent linearity for HfO<sub>2</sub> on nanowires [74]. It was also found that for dielectrics such as SiO<sub>2</sub>, self-assembled monolayers can improve the pH response linearity by lending additional surface groups with different dissociation constants [5]. It is worth noting here that some recent works have reported that certain structures such as dual-gated structures appear to increase the device surface sensitivity to exceed the Nernst limit [120], however, these structures rely on voltage amplification through capacitive coupling to achieve these super-Nernstian readouts, with the intrinsic sensitivity of the surface still below the Nernst limit.

**TABLE 1.** Examples of different types of Si-NW FETs as pH sensors at room temperature.

pH sensitivity (mV/pH)	pH range	Surface coating	Ref.
30	4-9	APTES on SiO <sub>2</sub>	[119]
48	7-10	SiO <sub>2</sub>	[76]
42-50	4-9	SiO <sub>2</sub>	[116]
50	2-9	APTES on SiO <sub>2</sub>	[117]
55.8 (nanowires) 51 (nanoplates)	4.3-10.5	HfO <sub>2</sub>	[74]
55.44±2.94	4-10	Al <sub>2</sub> O <sub>3</sub>	[61]
56±3	3-10	HfO <sub>2</sub> /Al <sub>2</sub> O <sub>3</sub>	[83]
57.8±1.2	2-10	Al <sub>2</sub> O <sub>3</sub>	[72]

Examples of applications of Si-NWs as pH sensors in monitoring biological activity include an electronic version of an Enzyme Linked ImmunoSorbent Assay (ELISA) [121], detection of antigen-specific T-cell activation [75], and monitoring of enzyme-substrate interactions [61]. A sensitive yet simpler, cheaper, and portable immunoassay platform can be created by replacing the fluorescence readout with Si nanoFET pH readout. T-cell antigen specificity of as

few as 200 cells can be tested in seconds by monitoring extracellular acidification using Si-NWs. In addition, Si nanoribbon based pH sensor has been used as a rapid enzyme FET through the detection of urea in phosphate buffered saline (PBS), and penicillinase in PBS and urine, at limits of detection of < 200 μM and 0.02 units/mL, respectively. The ability to extract accurate enzyme kinetics and the Michaelis–Menten constant (*K<sub>m</sub>*) from the acetylcholine-acetylcholinesterase reaction has also been demonstrated. While buffering in physiological systems can pose as a significant limitation to the measured response [61], pH-based detection of biological activity has benefits in repeatability, generalizability, simplicity of surface chemistry, and ability to overcome Debye-screening limitations.

### B. ION SENSING

In addition to pH sensing, which measures the activity of hydrogen ions, Si nanoFETs have also been used to detect the activity of other ions. Unlike with pH sensing, where bare dielectric surfaces are typically used for direct detection, sensing of other ionic species usually require functionalization with an ion-reactive or ion selective layer to impart specificity. Luo et al. used Si-NW FETs functionalized with 3-mercaptopropyltriethoxysilane to detect heavy-metal ions such as Hg<sup>2+</sup> and Cd<sup>2+</sup> at concentrations down to 10<sup>-7</sup> and 10<sup>-4</sup> M respectively. The device was shown to be minimally sensitive to other interfering metal cations including Mg<sup>2+</sup>, Ca<sup>2+</sup>, Cu<sup>2+</sup>, Co<sup>2+</sup>, Ni<sup>2+</sup>, Ba<sup>2+</sup>, K<sup>+</sup>, and Na<sup>+</sup> [122]. Bi et al. presented oligopeptide-modified Si-NW arrays to selectively detect Pb<sup>2+</sup> and Cu<sup>2+</sup> simultaneously, with detection limits of 1 nM and 10 nM, respectively [123]. To reduce interference from pH changes, Wipf et al. coated a thin film of gold over Al<sub>2</sub>O<sub>3</sub> passivated Si-NW FETs. They then demonstrated Na<sup>+</sup> sensing in a differential setup, by comparing the signal between a Si-NW functionalized with a self-assembled monolayer of thiol-modified crown ethers against a bare Si-NW. This setup was found to be selective against H<sup>+</sup>, K<sup>+</sup>, and Cl<sup>-</sup> [84].

### C. NUCLEIC ACIDS SENSING

Besides ion sensing, Si nanoFETs have been proven as highly sensitive potentiometric devices for direct charge sensing [124]. This is achieved by specific recognition and adsorption of charged biomolecules at the solution-dielectric interface, with the inherent charges on the target (bio)molecules shifting the surface potential and changing the current through the FET (Figure 4A).

Owing to the advantages of direct, ultra-sensitive, and label-free detection, Si nanoFETs promise to revolutionize the field of nucleic acids sensing. Femtomolar or lower detection limit (Table 2) has been achieved for detection of DNA hybridization. The upper bound on the dynamic range for analytes of ~20 mer in length is typically in the pM range [51], [125]. Herein, we aim to provide a short list of recent advances in nucleic acids detection based on CMOS compatible (or mostly compatible)



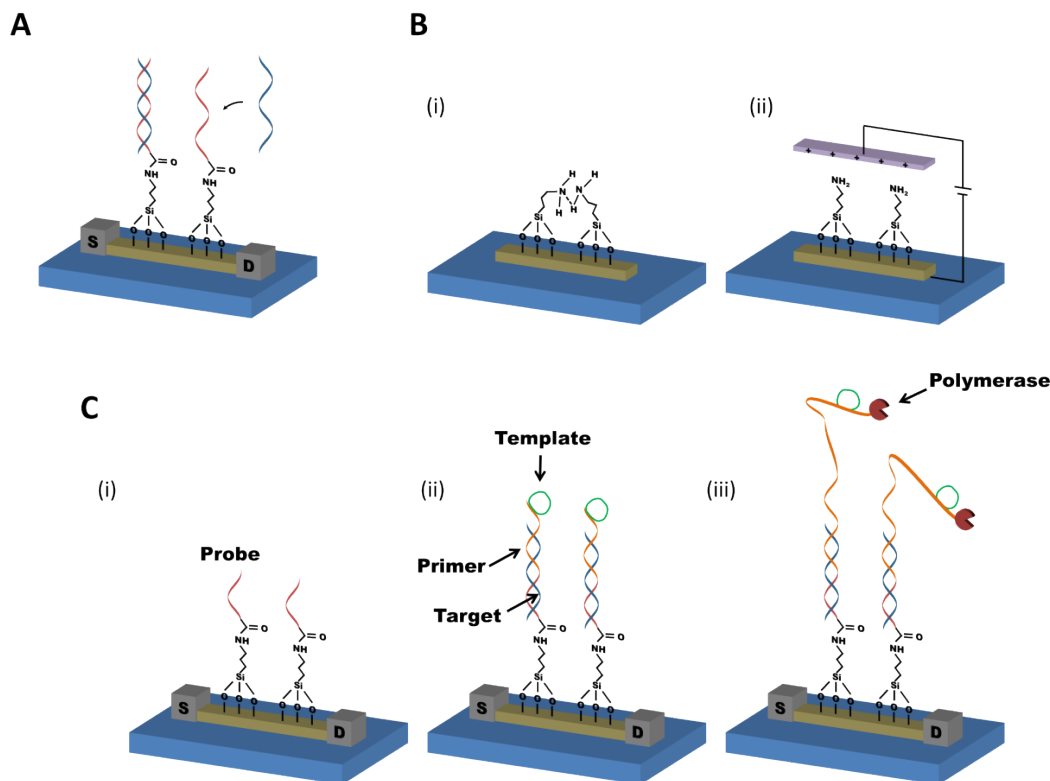


**FIGURE 4.** Methods of nucleic acid sensing using Si-NW FETs. (A) Schematic of nucleic acids sensing with Si-NW FET. (B) Electrical field alignment of APTES molecular structure. (C) Detection of DNA based on rolling circle amplification.

**TABLE 2.** A few examples of Si-NW FET nucleic acid sensors reported in the recent years.

Detection limit	Probe	Target	Year	Ref.
10 fM	PNA	ssDNA	2007	[125]
1 pM	ssDNA	ssDNA	2010	[132]
1 fM	ssDNA	ssDNA	2011	[51]
< 100 fM	ssDNA	ssDNA	2012	[74]
0.1 fM	ssDNA	ssDNA	2012	[128]
1 fM	ssDNA	ssDNA	2013	[131]
0.1 fM	ssDNA	ssDNA	2013	[129]
~ 0.1 fM	ssDNA	miRNA	2014	[52]

Si-NW FETs [51], [53], [56], [74], [79], [82], [104], [126]–[132]. The most common configuration for nucleic acid sensing is to immobilize one strand of nucleic acid on the surface of the Si-NW FET as receptor, and use that to detect its complementary strand in solution. Due to the high specificity of nucleic acid hybridization pairing and the high sensitivity of NWs, single nucleotide polymorphism can be easily distinguished using this method [128]. Owing to the phosphate groups on the nucleic acid backbone, DNA and RNA are highly negatively charged at physiological pH. Although they are well-suited as analytes due to their high negative charges, they make poor receptors due to both electrostatic repulsion with analytes and high background noise due to movement of bound probes

in solution. An important advancement in the field was thus the replacement of the negatively charged ssDNA probe with the neutrally charged PNA, which significantly improved DNA binding efficiency by minimizing electrostatic repulsion between the DNA analyte and the probe [126]. Gao et al. analyzed various factors (gate voltage, buffer ionic strength, and probe concentration) of their triangular Si-NW sensors and optimized the sensor performance for DNA sensing [128]. Chu et al. optimized their sensor by electrical field alignment of the APTES layer, which promoted the ssDNA probe arrangement on the surface and improved the sensor repeatability and sensitivity (Figure 4B) [129]. Efforts to further improve sensitivity was shown by Gao et al., where signal-to-noise ratio enhancement (>20) for DNA detection was accomplished through rolling circle amplification (Figure 4C). This created a long secondary ssDNA probe and increased the net negative charge of the nucleic acid sandwich on the surface, thus improving the signal [130]. Furthermore, detection of micro-RNA [53], and DNA methylation [127] have been reported as well. Lu et al. presented a Si-NW FET for rapid detection of micro-RNAs with a detection limit of ~600 copies in 8  $\mu$ L and excellent discrimination for single-nucleotide mismatch. To demonstrate clinical applicability of the device, the authors also analyzed micro-RNA in total RNA extracted from lung cancer cells and in total human serum samples. Maki et al. detected DNA methylation by capturing and concentrating

target DNA using magnetic beads, then testing the DNA using NW-FET functionalized with anti-5-methylcytosine molecule, which can capture methylated DNA. They were able to detect methylated DNA down to  $2.5 \times 10^{-19}$  mol in  $0.25 \mu\text{L}$  of concentrated solution. Nucleic acid sensing has also proven very useful in identification and detection of infectious diseases. Zhang et al. demonstrated a Si-NW FET based on PNA-DNA hybridization for sensitive detection of Dengue virus following RT-PCR amplification of a defining fragment in the capsid region [56]. Kao et al. designed an integrated microfluidic platform with Si-NW biosensors and a PCR module to detect the H1N1 2009 virus strain versus the seasonal influenza strain [104]. The PCR amplified nucleic acid products are directly flow downstream to be detected on the NWs.

Besides concentration quantification, affinity based detection (e.g. measuring receptor-analyte affinities and binding kinetics) has also been demonstrated by Si-NW FETs for DNA hybridizations [86] and protein-DNA interactions [82]. De et al. used a differential Si-NW setup to determine the equilibrium association constant of a 15-mer DNA to its complementary probe. The differential setup allowed for a  $30\times$  reduction in drift. Duan et al. determined the equilibrium dissociation constant ( $K_D \sim 10^{-7}$  M) between the HMGB1 protein and its ligand DNA. The real-time nature of the response allows  $k_{on}$  and  $k_{off}$  to be determined from the association and dissociation curves, respectively. To show that the NW FETs can be applied to measure molecules across a wide range of affinities, the same setup was used to determine the dissociation constant of the biotin-streptavidin interaction ( $K_D \sim 10^{-14}$  M).

Large-scale Si nanoFET sensor arrays for nucleic acid detection could provide useful applications in detection of infectious agents from cellular extracts, gene expression profiling and sequencing.

#### D. PROTEIN SENSING

Another biological analyte of significant interest is proteins, and CMOS-compatible Si-NW FETs have been used to detect small molecule-protein (e.g. biotin-Streptavidin [11], [82] and carbohydrate-protein [133]), in addition to DNA-protein interactions [134]. Similar devices have also been widely used as immunosensors for antigen detection [11], [55], [77], [135], [136]. Regardless of compatibility with CMOS processes, the most popular method for protein detection is to immobilize antibodies on the surface of the NW, and detect the intrinsic charge on the antigen as it binds to the antibody (Figure 5A).

Using this method, many different classes of proteins have been detected as analytes. The most popular biomarkers of interest include various disease biomarkers. For example, prostate specific antigen detection has been demonstrated on NW FETs by many groups due to its elevation in the presence of prostate cancer [96], [124], [137]. For cardiac markers, the main analyte of interest has been on cardiac Troponin I, due to its link to heart disorders [77], [80], [136].

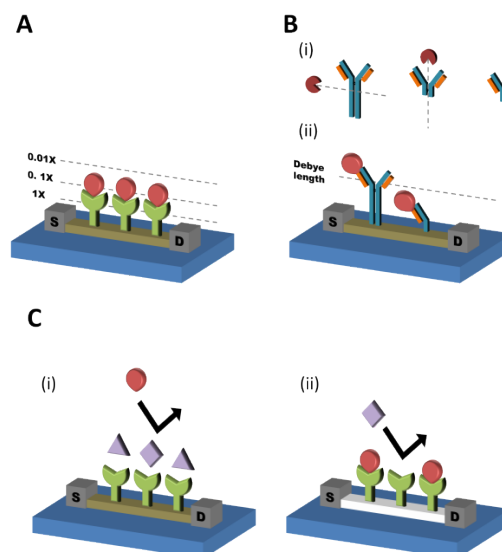


**FIGURE 5. Methods of protein sensing using Si-NW FETs. (A) Protein sensing using antibody receptors in buffer, Debye length increases with the reduction of buffer ionic strength. (B) Protein sensing using (i) antibody fragments cleaved from the whole antibody molecule, (ii) which allows the antigen to be brought within the Debye length. (C) NSB is blocked by the passivated surface.**

Raised Troponin levels are indicative of cardiac muscle damage and myocardial infarction. For many of these applications, detection limits in the femtomolar range has been reported in low ionic strength buffers. However, in real-world and clinically relevant applications, samples are rarely present in pure, low salt buffers. In fact, biological fluids such as whole blood are complex and abundant in salts and species of non-interest. Therefore, there are several major challenges that must be overcome before Si-NW FETs can be used directly for such samples and such applications.

Debye screening, the effect of bio-molecular charge screening by dissolved solution ions, is a phenomenon that significantly limits the sensitivity of Si-NW FETs in high ionic strength buffers [138]. The screening is enhanced exponentially in distance from the charged analyte to the NW surface, and is described by a characteristic length called the Debye length ( $\lambda_D$ ), given by

$$\lambda_D = \sqrt{\frac{\epsilon_0 \epsilon_r kT}{2N_A q^2 I}} \quad (8)$$

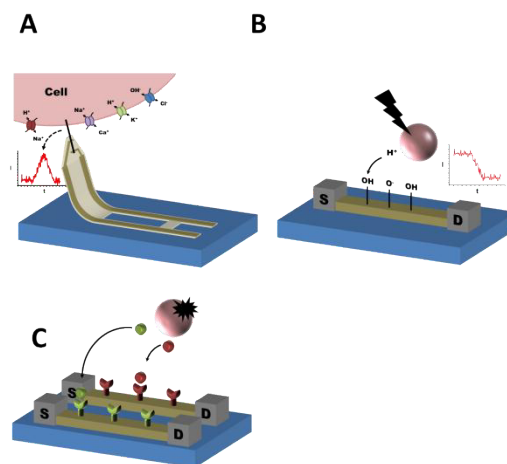
Where  $\epsilon_0$  is the vacuum permittivity,  $\epsilon_r$  is the relative permittivity of the medium,  $N_A$  is Avogadro's number, and  $I$  is the ionic strength of the buffer. In the case of nucleic acids, the receptors are relatively small and the analytes are highly charged, thus allowing for straightforward detection. However for proteins, the receptors (typically antibodies) are large compared to the Debye length in ionic solutions, thus the limitation of Debye screening is a major challenge. In Table 3, we summarize the Debye length in different concentrations of phosphate buffered saline at room temperature.

**TABLE 3.** Summary of Debye lengths for various ionic strength solutions.

PBS dilution	Salt concentration (mM)	Debye length (nm)
1x	150	0.7
0.1x	15	2.3
0.01x	1.5	7.3
0.001x	0.15	23

One can see that a solution to the issue is the reduction of buffer ionic strength, which will extend the Debye length. However, lowering the ionic strength requires complex desalting procedures, and may affect the stability and activity of various biological species. So far, the majority of the work in this area has been done with the protein of interest spiked into prepared low salt buffers or desalted biological fluids, and careful tuning of the buffer ionic strength is required [62], [133], [135]. An alternative method to reducing the ionic strength is to bring the antigen within the Debye length, which has been successfully demonstrated on bottom up NWs. A way to achieve this is to replace the large probe proteins with antibody fragments [80] or aptamers [139], which are relatively small and allow antigen binding to be detectable in physiological conditions. Elnathan et al. cleaved antibodies to obtain Fab portions, and used the fragments to sense troponin in high ionic strength solutions (Figure 5B). Using a moderate surface coverage of Fab fragments, cardiac troponin I was detected to a limit of <2 pM in 1× PBS [80]. Another way to bring antigens within the Debye length is to increase the Debye length itself. Recently, Gao et al. proposed a potential method for detecting proteins in high ionic strength solutions by incorporating a porous and biomolecule-permeable polyethylene glycol layer on the surface of the NW device [140]. The functionalized polymer layer increases the Debye screening length immediately adjacent to the device surface, and allowed a concentration dependent response to be obtained for PSA concentrations from 10-1000 nM.

Another important issue that must be overcome before Si-NW FETs can be used to directly detect biomarkers from the whole blood sample is the issue of nonspecific binding (NSB). Early studies were mainly focused on the detection of pure protein samples and only very limited research work has been directed toward biomarker detection directly from the blood or serum mainly because of challenges caused by protein NSB and complexity of the media. Chang et al. demonstrated a simple solution by passivation of the nanowire surface using Tween 20 to block the signal induced by NSB when performing active measurement in whole blood (Figure 5C) [141]. An approach that simultaneously addresses the Debye length problem and NSB has been reported by integrating a microfluidic filter chip with Si-NW FETs to achieve target biomarkers adsorption, separation and elution, which is subsequently detected by Si-NW FETs. This strategy is quite promising as

**FIGURE 6.** Methods of cell sensing using Si-NW FETs. (A) A bottom-up fabricated NW FET is inserted into a cell to record intracellular signals. (B) Detection of cellular activation via pH change. (C) Simultaneous detection of multiple cytokines with a dually functionalized Si-NW chip.

a point-of-care clinical diagnostics tool for whole blood samples (e.g. collected by a finger prick) [124].

### E. CELL SENSING

Micro/nanofabricated devices for the measurements of cellular metabolism e.g., pH change, gas exchange ( $O_2$ ,  $CO_2$ ), ion concentration, redox potential, and intracellular/extracellular potential are rapidly growing research fields [142], [143]. However, the negative effects of the larger devices on the cell proliferation and cytotoxicity and measurement repeatability are major challenges. Due to their relatively small size and footprint, NWs have the advantage of being minimally invasive towards the cell and are capable detection of at the single cell level. Both intracellular and extracellular activities have been recorded using Si-NWs and NW arrays. One special application of recording intracellular signals by penetration cell membranes has been achieved by bottom-up fabricated 3D-NW FETs which is rather challenging for top-down fabrication (Figure 6A) [144], [145]. In extracellular applications, both single Si-NW and NW arrays have been applied for the detection of extracellular bioelectricity from neurons and cardiomyocytes, detection of cellular activation via pH change (Figure 6B), simultaneous detection of multiple cytokines in response to various stimuli on one chip (Figure 6C), and determination of secretion kinetics of cytokines [55], [64], [75], [146], [147]. Extracellular cell sensing is an important application of CMOS-compatible NW-FETs, since the mass production of such devices can facilitate the monitoring of static states and/or dynamic evolution of biological process or reactions independently and simultaneously.

### V. LIMITATIONS AND SUMMARY

In the past few years, Si-NW FETs have shown the ability to detect a variety of biomolecules down to very low concentrations through potentiometric sensing. In this review, the operating principles, current methods for device

fabrication, fluid integration, surface functionalization, and performance limitations of Si-NW FETs have been summarized. Recent demonstrations of ion sensing, biomolecule detection and cellular function detection have been highlighted.

Many different techniques for fabricating different sized Si-NW FETs have been demonstrated thus far. CMOS-compatible fabrication processes which result in low noise interfaces are particularly promising due to their potential for low limits of detection, as well as facile electronic integration to create densely packed, multiplexed arrays. Device multiplexing is very useful in being able to collect large, statistically meaningful data sets on each analyte (including false positive and false negative rejection), while receptor multiplexing is very useful for the simultaneous detection of multiple analytes. Well-defined and uniform arrays additionally permit easy integration with fluidic delivery.

Two important performance metrics for any biosensor are the detection limit and the dynamic range. The SNR of the device (not the sensitivity) dictates the limit of detection, and the device dimensions that allow for optimal SNR depend on the application. Reducing device size improves charge sensitivity, so for applications such as studying single molecular binding kinetics, smaller devices have better SNR. However for diagnostic applications, larger device structures are better due to increased SNR. The upper bound on the dynamic range in concentration is limited by the device's ability to distinguish initial binding kinetics at high concentrations, whereas the lower bound is determined by the SNR. Device properties such as geometry, dielectric material, and functionalization need to be engineered according to the applications.

There are still several outstanding issues that need to be addressed to enable widespread adoption of this technology, foremost being charge screening for diagnostics under physiologic conditions, and simple and reliable reference electrode integration. Nonspecific molecular binding can be problematic for one-step affinity binding, but can be improved to have the same specificity as ELISAs by multistep binding strategies. The next stage for widespread adoption will be the validation of measurement reproducibility across laboratories and users, for which the low cost and portability of the approach is an advantage. A presently accepted technique for label-free detection is surface plasmon resonance (SPR), which is widely accepted due to its ability to provide convincing binding kinetics in addition to equilibrium data, giving confidence to the specificity of the detected signal. Si-NW FETs have the ability to provide the same information, with the additional advantages of low cost and integration, equipping it with the potential to be a disruptive technology in point of care diagnostics.

## REFERENCES

[1] J. R. De Courcera and R. Cavalieri, *Biosensors in Encyclopedia of Agricultural, Food, and Biological Engineering*. New York, NY, USA: Marcel Dekker, 2003.

- [2] K. S. Chang, C. C. Chen, J. T. Sheu, and Y.-K. Li, "Detection of an uncharged steroid with a silicon nanowire field-effect transistor," *Sens. Actuators B, Chem.*, vol. 138, no. 1, pp. 148–153, 2009.
- [3] C. S. Ah et al., "Detection of uncharged or feebly charged small molecules by field-effect transistor biosensors," *Biosensors Bioelectron.*, vol. 33, no. 1, pp. 233–240, 2012.
- [4] A. Jain, P. R. Nair, and M. A. Alam, "Flexure-FET biosensor to break the fundamental sensitivity limits of nanobiosensors using nonlinear electromechanical coupling," *Proc. Nat. Acad. Sci. USA*, vol. 109, no. 24, pp. 9304–9308, 2012.
- [5] Y. Cui, Q. Wei, H. Park, and C. M. Lieber, "Nanowire nanosensors for highly sensitive and selective detection of biological and chemical species," *Science*, vol. 293, no. 5533, pp. 1289–1292, 2001.
- [6] F. Patolsky, G. Zheng, and C. M. Lieber, "Nanowire-based biosensors," *Anal. Chem.*, vol. 78, no. 13, pp. 4260–4269, 2006.
- [7] A. K. Wanekaya, W. Chen, N. V. Myung, and A. Mulchandani, "Nanowire-based electrochemical biosensors," *Electroanalysis*, vol. 18, no. 6, pp. 533–550, 2006.
- [8] M. Curreli et al., "Real-time, label-free detection of biological entities using nanowire-based FETs," *IEEE Trans. Nanotechnol.*, vol. 7, no. 6, pp. 651–667, Nov. 2008.
- [9] O. H. Elibol, D. Morissette, D. Akin, J. P. Denton, and R. Bashir, "Integrated nanoscale silicon sensors using top-down fabrication," *Appl. Phys. Lett.*, vol. 83, no. 22, pp. 4613–4615, 2003.
- [10] Z. Li, Y. Chen, X. Li, T. I. Kamins, K. Nauka, and R. S. Williams, "Sequence-specific label-free DNA sensors based on silicon nanowires," *Nano Lett.*, vol. 4, no. 2, pp. 245–247, 2004.
- [11] E. Stern et al., "Label-free immunodetection with CMOS-compatible semiconducting nanowires," *Nature*, vol. 445, pp. 519–522, Feb. 2007.
- [12] B. L. Allen, P. D. Kichambare, and A. Star, "Carbon nanotube field-effect-transistor-based biosensors," *Adv. Mater.*, vol. 19, no. 11, pp. 1439–1451, 2007.
- [13] S. Sorgenfrei et al., "Label-free single-molecule detection of DNA-hybridization kinetics with a carbon nanotube field-effect transistor," *Nature Nanotechnol.*, vol. 6, pp. 126–132, Jan. 2011.
- [14] S. Liu and X. Guo, "Carbon nanomaterials field-effect-transistor-based biosensors," *NPG Asia Mater.*, vol. 4, p. e23, Aug. 2012.
- [15] Y. Yun et al., "Nanotube electrodes and biosensors," *Nano Today*, vol. 2, no. 6, pp. 30–37, 2007.
- [16] D. R. Kauffman and A. Star, "Carbon nanotube gas and vapor sensors," *Angew. Chem. Int. Ed.*, vol. 47, no. 35, pp. 6550–6570, 2008.
- [17] T. Zhang, S. Mubeen, N. V. Myung, and M. A. Deshusses, "Recent progress in carbon nanotube-based gas sensors," *Nanotechnology*, vol. 19, no. 33, p. 332001, 2008.
- [18] C. M. Hangarter, M. Bangar, A. Mulchandani, and N. V. Myung, "Conducting polymer nanowires for chemiresistive and FET-based bio/chemical sensors," *J. Mater. Chem.*, vol. 20, no. 16, pp. 3131–3140, 2010.
- [19] L. M. Bellan, D. Wu, and R. S. Langer, "Current trends in nanobiosensor technology," *Wiley Interdiscipl. Rev., Nanomed. Nanobiotechnol.*, vol. 3, no. 3, pp. 229–246, 2011.
- [20] A. L. Briseno, S. C. B. Mannsfeld, S. A. Jenekhe, Z. Bao, and Y. Xia, "Introducing organic nanowire transistors," *Mater. Today*, vol. 11, no. 4, pp. 38–47, 2008.
- [21] A. Mulchandani and N. V. Myung, "Conducting polymer nanowires-based label-free biosensors," *Current Opinion Biotechnol.*, vol. 22, no. 4, pp. 502–508, 2011.
- [22] F. Schwierz, "Graphene transistors," *Nature Nanotechnol.*, vol. 5, no. 7, pp. 487–496, 2010.
- [23] P. K. Ang, W. Chen, A. T. S. Wee, and K. P. Loh, "Solution-gated epitaxial graphene as pH sensor," *J. Amer. Chem. Soc.*, vol. 130, no. 44, pp. 14392–14393, 2008.
- [24] Y. Ohno, K. Maehashi, Y. Yamashiro, and K. Matsumoto, "Electrolyte-gated graphene field-effect transistors for detecting pH and protein adsorption," *Nano Lett.*, vol. 9, no. 9, pp. 3318–3322, 2009.
- [25] W. Fu et al., "Graphene transistors are insensitive to pH changes in solution," *Nano Lett.*, vol. 11, no. 9, pp. 3597–3600, 2011.
- [26] S. Mao, G. Lu, K. Yu, Z. Bo, and J. Chen, "Specific protein detection using thermally reduced graphene oxide sheet decorated with gold nanoparticle-antibody conjugates," *Adv. Mater.*, vol. 22, no. 32, pp. 3521–3526, 2010.
- [27] Y. Ohno, K. Maehashi, and K. Matsumoto, "Label-free biosensors based on aptamer-modified graphene field-effect transistors," *J. Amer. Chem. Soc.*, vol. 132, no. 51, pp. 18012–18013, 2010.

- [28] N. Mohanty and V. Berry, "Graphene-based single-bacterium resolution biodevice and DNA transistor: Interfacing graphene derivatives with nanoscale and microscale biocomponents," *Nano Lett.*, vol. 8, no. 12, pp. 4469–4476, 2008.
- [29] X. Dong, Y. Shi, W. Huang, P. Chen, and L.-J. Li, "Electrical detection of DNA hybridization with single-base specificity using transistors based on CVD-grown graphene sheets," *Adv. Mater.*, vol. 22, no. 14, pp. 1649–1653, 2010.
- [30] B. Cai, S. Wang, L. Huang, Y. Ning, Z. Zhang, and G.-J. Zhang, "Ultra-sensitive label-free detection of PNA–DNA hybridization by reduced graphene oxide field-effect transistor biosensor," *ACS Nano*, vol. 8, no. 3, pp. 2632–2638, 2014.
- [31] Y. Huang, X. Dong, Y. Shi, C. M. Li, L.-J. Li, and P. Chen, "Nanoelectronic biosensors based on CVD grown graphene," *Nanoscale*, vol. 2, no. 8, pp. 1485–1488, 2010.
- [32] T. Cohen-Karni, Q. Qing, Q. Li, Y. Fang, and C. M. Lieber, "Graphene and nanowire transistors for cellular interfaces and electrical recording," *Nano Lett.*, vol. 10, no. 3, pp. 1098–1102, 2010.
- [33] D. Sarkar, W. Liu, X. Xie, A. C. Anselmo, S. Mitragotri, and K. Banerjee, "MoS<sub>2</sub> field-effect transistor for next-generation label-free biosensors," *ACS Nano*, vol. 8, no. 4, pp. 3992–4003, 2014.
- [34] G. Jegerszki, Á. Takács, I. Bitter, and R. E. Gyurcsányi, "Solid-state ion channels for potentiometric sensing," *Angew. Chem.*, vol. 123, no. 7, pp. 1694–1697, 2011.
- [35] T. Yin and W. Qin, "Applications of nanomaterials in potentiometric sensors," *TrAC Trends Anal. Chem.*, vol. 51, pp. 79–86, Nov. 2013.
- [36] J. Ampurdanés, G. A. Crespo, A. Maroto, M. A. Sarmentero, P. Ballester, and F. X. Rius, "Determination of choline and derivatives with a solid-contact ion-selective electrode based on octaamide cavitand and carbon nanotubes," *Biosensors Bioelectron.*, vol. 25, no. 2, pp. 344–349, 2009.
- [37] G. A. Crespo, D. Guga, S. Macho, and F. X. Rius, "Solid-contact pH-selective electrode using multi-walled carbon nanotubes," *Anal. Bioanal. Chem.*, vol. 395, no. 7, pp. 2371–2376, 2009.
- [38] E. Jaworska, M. Wójcik, A. Kisiel, J. Mieczkowski, and A. Michalska, "Gold nanoparticles solid contact for ion-selective electrodes of highly stable potential readings," *Talanta*, vol. 85, no. 4, pp. 1986–1989, 2011.
- [39] J. L. Arlett, E. B. Myers, and M. L. Roukes, "Comparative advantages of mechanical biosensors," *Nature Nanotechnol.*, vol. 6, pp. 203–215, Mar. 2011.
- [40] R. S. Wagner and W. C. Ellis, "Vapor-liquid-solid mechanism of single crystal growth," *Appl. Phys. Lett.*, vol. 4, no. 5, pp. 89–90, 1964.
- [41] Y. Huang, X. Duan, Q. Wei, and C. M. Lieber, "Directed assembly of one-dimensional nanostructures into functional networks," *Science*, vol. 291, no. 5504, pp. 630–633, 2001.
- [42] D. Whang, S. Jin, Y. Wu, and C. M. Lieber, "Large-scale hierarchical organization of nanowire arrays for integrated nanosystems," *Nano Lett.*, vol. 3, no. 9, pp. 1255–1259, 2003.
- [43] S. Jin, D. Whang, M. C. McAlpine, R. S. Friedman, Y. Wu, and C. M. Lieber, "Scalable interconnection and integration of nanowire devices without registration," *Nano Lett.*, vol. 4, no. 5, pp. 915–919, 2004.
- [44] G. Yu, A. Cao, and C. M. Lieber, "Large-area blown bubble films of aligned nanowires and carbon nanotubes," *Nature Nanotechnol.*, vol. 2, pp. 372–377, May 2007.
- [45] Z. Fan *et al.*, "Wafer-scale assembly of highly ordered semiconductor nanowire arrays by contact printing," *Nano Lett.*, vol. 8, no. 1, pp. 20–25, 2008.
- [46] L. Dong *et al.*, "Dielectrophoretically controlled fabrication of single-crystal nickel silicide nanowire interconnects," *Nano Lett.*, vol. 5, no. 10, pp. 2112–2115, 2005.
- [47] S. Raychaudhuri, S. A. Dayeh, D. Wang, and E. T. Yu, "Precise semiconductor nanowire placement through dielectrophoresis," *Nano Lett.*, vol. 9, no. 6, pp. 2260–2266, 2009.
- [48] E. M. Freer, O. Grachev, X. Duan, S. Martin, and D. P. Stumbo, "High-yield self-limiting single-nanowire assembly with dielectrophoresis," *Nature Nanotechnol.*, vol. 5, pp. 525–530, Jun. 2010.
- [49] I. Park, Z. Li, A. P. Pisano, and R. S. Williams, "Top-down fabricated silicon nanowire sensors for real-time chemical detection," *Nanotechnology*, vol. 21, no. 1, p. 015501, 2010.
- [50] A. Tarasov *et al.*, "True reference nanosensor realized with silicon nanowires," *Langmuir*, vol. 28, no. 25, pp. 9899–9905, 2012.
- [51] A. Gao *et al.*, "Silicon-nanowire-based CMOS-compatible field-effect transistor nanosensors for ultrasensitive electrical detection of nucleic acids," *Nano Lett.*, vol. 11, no. 9, pp. 3974–3978, 2011.
- [52] N. Lu *et al.*, "Ultra-sensitive nucleic acids detection with electrical nanosensors based on CMOS-compatible silicon nanowire field-effect transistors," *Methods*, vol. 63, no. 3, pp. 212–218, 2013.
- [53] N. Lu *et al.*, "CMOS-compatible silicon nanowire field-effect transistors for ultrasensitive and label-free microRNAs sensing," *Small*, vol. 10, no. 10, pp. 2022–2028, 2014.
- [54] R. Juhasz, N. Elfström, and J. Linnros, "Controlled fabrication of silicon nanowires by electron beam lithography and electrochemical size reduction," *Nano Lett.*, vol. 5, no. 2, pp. 275–280, 2005.
- [55] T.-S. Pui, A. Agarwal, F. Ye, Z.-Q. Tou, Y. Huang, and P. Chen, "Ultra-sensitive detection of adipocytokines with CMOS-compatible silicon nanowire arrays," *Nanoscale*, vol. 1, no. 1, pp. 159–163, 2009.
- [56] G.-J. Zhang *et al.*, "Silicon nanowire biosensor for highly sensitive and rapid detection of dengue virus," *Sens. Actuators B, Chem.*, vol. 146, no. 1, pp. 138–144, 2010.
- [57] S. Chen, J. G. Bomer, W. G. van der Wiel, E. T. Carlen, and A. van den Berg, "Top-down fabrication of sub-30 nm monocrystalline silicon nanowires using conventional microfabrication," *ACS Nano*, vol. 3, no. 11, pp. 3485–3492, 2009.
- [58] N. K. Rajan, D. A. Routenberg, J. Chen, and M. A. Reed, "1/f noise of silicon nanowire BioFETs," *IEEE Electron Device Lett.*, vol. 31, no. 6, pp. 615–617, Jun. 2010.
- [59] B. Reddy, Jr., *et al.*, "High-*k* dielectric Al<sub>2</sub>O<sub>3</sub> nanowire and nanoplate field effect sensors for improved pH sensing," *Biomed. Microdevices*, vol. 13, no. 2, pp. 335–344, 2011.
- [60] N. Elfström, A. E. Karlström, and J. Linnros, "Silicon nanoribbons for electrical detection of biomolecules," *Nano Lett.*, vol. 8, no. 3, pp. 945–949, Mar. 2008.
- [61] L. Mu, I. A. Droujinine, N. K. Rajan, S. D. Sawtelle, and M. A. Reed, "Direct, rapid, and label-free detection of enzyme-substrate interactions in physiological buffers using CMOS-compatible nanoribbon sensors," *Nano Lett.*, vol. 14, no. 9, pp. 5315–5322, 2014.
- [62] M. M. Hakim *et al.*, "Thin film polycrystalline silicon nanowire biosensors," *Nano Lett.*, vol. 12, no. 4, pp. 1868–1872, 2012.
- [63] C.-H. Lin, C.-H. Hung, C.-Y. Hsiao, H.-C. Lin, F.-H. Ko, and Y.-S. Yang, "Poly-silicon nanowire field-effect transistor for ultrasensitive and label-free detection of pathogenic avian influenza DNA," *Biosensors Bioelectron.*, vol. 24, no. 10, pp. 3019–3024, 2009.
- [64] T. S. Pui, A. Agarwal, F. Ye, N. Balasubramanian, and P. Chen, "CMOS-compatible nanowire sensor arrays for detection of cellular bioelectricity," *Small*, vol. 5, no. 2, pp. 208–212, 2009.
- [65] S. Rigante *et al.*, "Sensing with advanced computing technology: Fin field effect transistors with high-*k* gate stack on bulk silicon," *ACS Nano*, 2015.
- [66] A. Gao, N. Lu, P. Dai, C. Fan, Y. Wang, and T. Li, "Direct ultrasensitive electrical detection of prostate cancer biomarkers with CMOS-compatible n- and p-type silicon nanowire sensor arrays," *Nanoscale*, vol. 6, no. 21, pp. 13036–13042, 2014.
- [67] M.-C. Chen *et al.*, "A CMOS-compatible poly-Si nanowire device with hybrid sensor/memory characteristics for system-on-chip applications," *Sensors*, vol. 12, no. 4, pp. 3952–3963, 2012.
- [68] C. W. Huang *et al.*, "A CMOS wireless biomolecular sensing system-on-chip based on polysilicon nanowire technology," *Lab Chip*, vol. 13, no. 22, pp. 4451–4459, 2013.
- [69] A. Vacic, J. M. Criscione, E. Stern, N. K. Rajan, T. Fahmy, and M. A. Reed, "Calibration methods for silicon nanowire BioFETs," in *Proc. Int. Conf. Microelectron. Test Struct. (ICMTS)*, Mar. 2014, pp. 203–206.
- [70] H.-J. Jang, M.-S. Kim, and W.-J. Cho, "Development of engineered sensing membranes for field-effect ion-sensitive devices based on stacked high-*k* dielectric layers," *IEEE Electron Device Lett.*, vol. 32, no. 7, pp. 973–975, Jul. 2011.
- [71] T.-E. Bae, H.-J. Jang, J.-H. Yang, and W.-J. Cho, "High performance of silicon nanowire-based biosensors using a high-*k* stacked sensing thin film," *ACS Appl. Mater. Interf.*, vol. 5, no. 11, pp. 5214–5218, 2013.
- [72] S. Chen, J. G. Bomer, E. T. Carlen, and A. van den Berg, "Al<sub>2</sub>O<sub>3</sub>/silicon nanoISFET with near ideal Nernstian response," *Nano Lett.*, vol. 11, no. 6, pp. 2334–2341, 2011.
- [73] S. Zafar, C. D'Emic, A. Afzali, B. Fletcher, Y. Zhu, and T. Ning, "Optimization of pH sensing using silicon nanowire field effect transistors with HfO<sub>2</sub> as the sensing surface," *Nanotechnology*, vol. 22, no. 40, p. 405501, 2011.

- [74] B. R. Dorvel et al., "Silicon nanowires with high- $k$  hafnium oxide dielectrics for sensitive detection of small nucleic acid oligomers," *ACS Nano*, vol. 6, no. 7, pp. 6150–6164, 2012.
- [75] E. Stern, E. R. Steenblock, M. A. Reed, and T. M. Fahmy, "Label-free electronic detection of the antigen-specific T-cell immune response," *Nano Lett.*, vol. 8, no. 10, pp. 3310–3314, 2008.
- [76] A. De, J. van Nieuwkastele, E. T. Carlen, and A. van den Berg, "Integrated label-free silicon nanowire sensor arrays for (bio)chemical analysis," *Analyst*, vol. 138, no. 11, pp. 3221–3229, 2013.
- [77] J. H. Chua, R.-E. Chee, A. Agarwal, S. M. Wong, and G.-J. Zhang, "Label-free electrical detection of cardiac biomarker with complementary metal-oxide semiconductor-compatible silicon nanowire sensor arrays," *Anal. Chem.*, vol. 81, no. 15, pp. 6266–6271, 2009.
- [78] D. R. Kim, C. H. Lee, and X. Zheng, "Probing flow velocity with silicon nanowire sensors," *Nano Lett.*, vol. 9, no. 5, pp. 1984–1988, 2009.
- [79] M. Chiesa et al., "Detection of the early stage of recombinational DNA repair by silicon nanowire transistors," *Nano Lett.*, vol. 12, no. 3, pp. 1275–1281, 2012.
- [80] R. Elnathan et al., "Biorecognition layer engineering: Overcoming screening limitations of nanowire-based FET devices," *Nano Lett.*, vol. 12, no. 10, pp. 5245–5254, 2012.
- [81] T.-Y. Lin et al., "Improved silicon nanowire field-effect transistors for fast protein-protein interaction screening," *Lab Chip*, vol. 13, no. 4, pp. 676–684, 2013.
- [82] X. Duan, Y. Li, N. K. Rajan, D. A. Routenberg, Y. Modis, and M. A. Reed, "Quantification of the affinities and kinetics of protein interactions using silicon nanowire biosensors," *Nature Nanotechnol.*, vol. 7, pp. 401–407, May 2012.
- [83] A. Tarasov et al., "Understanding the electrolyte background for biochemical sensing with ion-sensitive field-effect transistors," *ACS Nano*, vol. 6, no. 10, pp. 9291–9298, 2012.
- [84] M. Wipf et al., "Selective sodium sensing with gold-coated silicon nanowire field-effect transistors in a differential setup," *ACS Nano*, vol. 7, no. 7, pp. 5978–5983, 2013.
- [85] S. Kim et al., "Silicon nanowire ion sensitive field effect transistor with integrated Ag/AgCl electrode: pH sensing and noise characteristics," *Analyst*, vol. 136, no. 23, pp. 5012–5016, 2011.
- [86] Y. L. Bunimovich, Y. S. Shin, W.-S. Yeo, M. Amori, G. Kwong, and J. R. Heath, "Quantitative real-time measurements of DNA hybridization with alkylated nonoxidized silicon nanowires in electrolyte solution," *J. Amer. Chem. Soc.*, vol. 128, no. 50, pp. 16323–16331, 2006.
- [87] X. Duan, N. K. Rajan, M. H. Izadi, and M. A. Reed, "Complementary metal oxide semiconductor-compatible silicon nanowire biofield-effect transistors as affinity biosensors," *Nanomedicine*, vol. 8, no. 11, pp. 1839–1851, 2013.
- [88] L. C. P. M. de Smet, D. Ullien, E. J. R. Sudhölter, and M. Mescher, *Organic Surface Modification of Silicon Nanowire-Based Sensor Devices*. Rijeka, Croatia: InTech, 2011.
- [89] B. Dorvel, B. Reddy, Jr., and R. Bashir, "Effect of biointerfacing linker chemistries on the sensitivity of silicon nanowires for protein detection," *Anal. Chem.*, vol. 85, no. 20, pp. 9493–9500, Oct. 2013.
- [90] S.-P. Lin, T.-Y. Chi, T.-Y. Lai, and M.-C. Liu, "The effect of varied functional biointerfaces on the sensitivity of silicon nanowire MOSFET," in *Proc. IEEE EMBS Conf. Biomed. Eng. Sci. (IECBES)*, Dec. 2012, pp. 162–166.
- [91] B. Dorvel et al., "Vapor-phase deposition of monofunctional alkoxy-silanes for sub-nanometer-level biointerfacing on silicon oxide surfaces," *Adv. Funct. Mater.*, vol. 20, no. 1, pp. 87–95, 2010.
- [92] R. Ermanok, O. Assad, K. Zigelboim, B. Wang, and H. Haick, "Discriminative power of chemically sensitive silicon nanowire field effect transistors to volatile organic compounds," *ACS Appl. Mater. Interf.*, vol. 5, no. 21, pp. 11172–11183, 2013.
- [93] X. Duan, N. K. Rajan, D. A. Routenberg, J. Huskens, and M. A. Reed, "Regenerative electronic biosensors using supramolecular approaches," *ACS Nano*, vol. 7, no. 5, pp. 4014–4021, 2013.
- [94] X. Duan et al., "Functionalized polyelectrolytes assembling on nano-BioFETs for biosensing applications," *Adv. Funct. Mater.*, vol. 25, no. 15, pp. 2279–2286, 2015.
- [95] Y. Engel, R. Elnathan, A. Pevzner, G. Davidi, E. Flaxer, and F. Patolsky, "Supersensitive detection of explosives by silicon nanowire arrays," *Angew. Chem. Int. Ed.*, vol. 49, no. 38, pp. 6830–6835, 2010.
- [96] G. Zheng, F. Patolsky, Y. Cui, W. U. Wang, and C. M. Lieber, "Multiplexed electrical detection of cancer markers with nanowire sensor arrays," *Nature Biotechnol.*, vol. 23, pp. 1294–1301, Sep. 2005.
- [97] G.-J. Zhang, Z. H. H. Luo, M. J. Huang, J. J. Ang, T. G. Kang, and H. Ji, "An integrated chip for rapid, sensitive, and multiplexed detection of cardiac biomarkers from fingerprick blood," *Biosensors Bioelectron.*, vol. 28, no. 1, pp. 459–463, 2011.
- [98] I. Park, Z. Li, A. P. Pisano, and R. S. Williams, "Selective surface functionalization of silicon nanowires via nanoscale Joule heating," *Nano Lett.*, vol. 7, no. 10, pp. 3106–3111, 2007.
- [99] E. Stern et al., "Electropolymerization on microelectrodes: Functionalization technique for selective protein and DNA conjugation," *Anal. Chem.*, vol. 78, no. 18, pp. 6340–6346, 2006.
- [100] Y. L. Bunimovich, G. Ge, K. C. Beverly, R. S. Ries, L. Hood, and J. R. Heath, "Electrochemically programmed, spatially selective biofunctionalization of silicon wires," *Langmuir*, vol. 20, no. 4, pp. 10630–10638, 2004.
- [101] J.-H. Lim, D. S. Ginger, K.-B. Lee, J. Heo, J.-M. Nam, and C. A. Mirkin, "Direct-write dip-pen nanolithography of proteins on modified silicon oxide surfaces," *Angew. Chem. Int. Ed.*, vol. 42, no. 20, pp. 2309–2312, May 2003.
- [102] G.-J. Zhang et al., "Multiplexed detection of cardiac biomarkers in serum with nanowire arrays using readout ASIC," *Biosensors Bioelectron.*, vol. 35, no. 1, pp. 218–223, May 2012.
- [103] A. Kim et al., "Direct label-free electrical immunodetection in human serum using a flow-through-apparatus approach with integrated field-effect transistors," *Biosensors Bioelectron.*, vol. 25, no. 7, pp. 1767–1773, Mar. 2010.
- [104] L. T.-H. Kao et al., "Multiplexed detection and differentiation of the DNA strains for influenza A (H1N1 2009) using a silicon-based microfluidic system," *Biosensors Bioelectron.*, vol. 26, no. 5, pp. 2006–2011, Jan. 2011.
- [105] K. J. Albert et al., "Cross-reactive chemical sensor arrays," *Chem. Rev.*, vol. 100, no. 7, pp. 2595–2626, 2000.
- [106] A. Cao, E. J. R. Sudhölter, and L. C. P. M. de Smet, "Silicon nanowire-based devices for gas-phase sensing," *Sensors*, vol. 14, no. 1, pp. 245–271, Jan. 2013.
- [107] B. Wang, J. C. Cancilla, J. S. Torrecilla, and H. Haick, "Artificial sensing intelligence with silicon nanowires for ultrasensitive detection in the gas phase," *Nano Lett.*, vol. 14, no. 2, pp. 933–938, Jan. 2014.
- [108] P. R. Nair and M. A. Alam, "Performance limits of nanobiosensors," *Appl. Phys. Lett.*, vol. 88, no. 3, p. 233120, Jun. 2006.
- [109] N. K. Rajan, X. Duan, and M. A. Reed, "Performance limitations for nanowire/nanoribbon biosensors," *Nanomed. Nanobiotechnol.*, vol. 5, no. 6, pp. 629–645, Nov. 2013.
- [110] R. Jayaraman and C. G. Sodini, "A  $1/f$  noise technique to extract the oxide trap density near the conduction band edge of silicon," *IEEE Trans. Electron Devices*, vol. 36, no. 8, pp. 1773–1782, Sep. 1989.
- [111] N. K. Rajan, D. A. Routenberg, and M. A. Reed, "Optimal signal-to-noise ratio for silicon nanowire biochemical sensors," *Appl. Phys. Lett.*, vol. 98, no. 26, p. 264107, Jun. 2011.
- [112] K. Bedner et al., "Investigation of the dominant  $1/f$  noise source in silicon nanowire sensors," *Sens. Actuators B, Chem.*, vol. 191, pp. 270–275, Feb. 2014.
- [113] N. K. Rajan, K. Brower, X. Duan, and M. A. Reed, "Limit of detection of field effect transistor biosensors: Effects of surface modification and size dependence," *Appl. Phys. Lett.*, vol. 104, no. 8, p. 084106, Feb. 2014.
- [114] V. S. Mahajan and P. Jarolim, "How to interpret elevated cardiac troponin levels," *Circulation*, vol. 124, no. 21, pp. 2350–2354, Nov. 2011.
- [115] P. Bergveld, "Thirty years of ISFETOLOGY: What happened in the past 30 years and what may happen in the next 30 years," *Sens. Actuators B, Chem.*, vol. 88, no. 1, pp. 1–20, Jan. 2003.
- [116] X. T. Vu, R. Stockmann, B. Wolfrum, A. Offenhäuser, and S. Ingebrandt, "Fabrication and application of a microfluidic-embedded silicon nanowire biosensor chip," *Phys. Status Solidi A*, vol. 207, no. 4, pp. 850–857, Apr. 2010.
- [117] R. Tian, S. Regonda, J. Gao, Y. Liu, and W. Hu, "Ultrasensitive protein detection using lithographically defined Si multi-nanowire field effect transistors," *Lab Chip*, vol. 11, no. 11, pp. 1952–1961, Apr. 2011.
- [118] S. Choi, I. Park, Z. Hao, H.-Y. N. Holman, and A. P. Pisano, "Quantitative studies of long-term stable, top-down fabricated silicon nanowire pH sensors," *Appl. Phys. A*, vol. 107, no. 2, pp. 421–428, May 2012.
- [119] X. P. A. Gao, G. Zheng, and C. M. Lieber, "Subthreshold regime has the optimal sensitivity for nanowire FET biosensors," *Nano Lett.*, vol. 10, no. 2, pp. 547–552, Nov. 2009.
- [120] O. Knopfmacher et al., "Nernst limit in dual-gated Si-nanowire FET sensors," *Nano Lett.*, vol. 10, no. 6, pp. 2268–2274, May 2010.

- [121] E. Stern *et al.*, “A nanoelectronic enzyme-linked immunosorbent assay for detection of proteins in physiological solutions,” *Small*, vol. 6, no. 2, pp. 232–238, Jan. 2010.
- [122] L. Luo *et al.*, “Silicon nanowire sensors for  $Hg^{2+}$  and  $Cd^{2+}$  ions,” *Appl. Phys. Lett.*, vol. 94, no. 19, pp. 193101-1–193101-3, 2009.
- [123] X. Bi, A. Agarwal, and K.-L. Yang, “Oligopeptide-modified silicon nanowire arrays as multichannel metal ion sensors,” *Biosensors Bioelectron.*, vol. 24, no. 11, pp. 3248–3251, Jul. 2009.
- [124] E. Stern *et al.*, “Label-free biomarker detection from whole blood,” *Nature Nanotechnol.*, vol. 5, no. 2, pp. 138–142, 2010.
- [125] Z. Gao *et al.*, “Silicon nanowire arrays for label-free detection of DNA,” *Anal. Chem.*, vol. 79, no. 9, pp. 3291–3297, Apr. 2007.
- [126] A. Cattani-Scholz *et al.*, “Organophosphonate-based PNA-functionalization of silicon nanowires for label-free DNA detection,” *ACS Nano*, vol. 2, no. 8, pp. 1653–1660, Jul. 2008.
- [127] W. C. Maki, N. N. Mishra, E. G. Cameron, B. Filanoski, S. K. Rastogi, and G. K. Maki, “Nanowire-transistor based ultra-sensitive DNA methylation detection,” *Biosensors Bioelectron.*, vol. 23, no. 6, pp. 780–787, Jan. 2008.
- [128] A. Gao *et al.*, “Enhanced sensing of nucleic acids with silicon nanowire field effect transistor biosensors,” *Nano Lett.*, vol. 12, no. 10, pp. 5262–5268, Sep. 2012.
- [129] C.-J. Chu *et al.*, “Improving nanowire sensing capability by electrical field alignment of surface probing molecules,” *Nano Lett.*, vol. 13, no. 6, pp. 2564–2569, May 2013.
- [130] A. Gao *et al.*, “Signal-to-noise ratio enhancement of silicon nanowires biosensor with rolling circle amplification,” *Nano Lett.*, vol. 13, no. 9, pp. 4123–4130, Aug. 2013.
- [131] G. Wenga, E. Jacques, A.-C. Salaün, R. Rogel, L. Pichon, and F. Geneste, “Step-gate polysilicon nanowires field effect transistor compatible with CMOS technology for label-free DNA biosensor,” *Biosensors Bioelectron.*, vol. 40, no. 1, pp. 141–146, Feb. 2013.
- [132] S.-W. Ryu *et al.*, “Gold nanoparticle embedded silicon nanowire biosensor for applications of label-free DNA detection,” *Biosensors Bioelectron.*, vol. 25, no. 9, pp. 2182–2185, May 2010.
- [133] G.-J. Zhang, M. J. Huang, J. J. Ang, Q. Yao, and Y. Ning, “Label-free detection of carbohydrate–protein interactions using nanoscale field-effect transistor biosensors,” *Anal. Chem.*, vol. 85, no. 9, pp. 4392–4397, Apr. 2013.
- [134] G.-J. Zhang *et al.*, “Highly sensitive and reversible silicon nanowire biosensor to study nuclear hormone receptor protein and response element DNA interactions,” *Biosensors Bioelectron.*, vol. 26, no. 2, pp. 365–370, Oct. 2010.
- [135] D. P. Tran *et al.*, “Complementary metal oxide semiconductor compatible silicon nanowires-on-a-chip: Fabrication and preclinical validation for the detection of a cancer prognostic protein marker in serum,” *Anal. Chem.*, vol. 87, no. 3, pp. 1662–1668, Feb. 2015.
- [136] T. Kong, R. Su, B. Zhang, Q. Zhang, and G. Cheng, “CMOS-compatible, label-free silicon-nanowire biosensors to detect cardiac troponin I for acute myocardial infarction diagnosis,” *Biosensors Bioelectron.*, vol. 34, no. 1, pp. 267–272, Apr. 2012.
- [137] Y.-W. Huang *et al.*, “Real-time and label-free detection of the prostate-specific antigen in human serum by a polycrystalline silicon nanowire field-effect transistor biosensor,” *Anal. Chem.*, vol. 85, no. 16, pp. 7912–7918, Jul. 2013.
- [138] E. Stern, R. Wagner, F. J. Sigworth, R. Breaker, T. M. Fahmy, and M. A. Reed, “Importance of the Debye screening length on nanowire field effect transistor sensors,” *Nano Lett.*, vol. 7, no. 11, pp. 3405–3409, Oct. 2007.
- [139] X. T. Cui, X. Luo, I. Lee, J. Huang, and M. Yun, “Ultrasensitive protein detection using an aptamer-functionalized single polyaniline nanowire,” *Chem. Commun.*, vol. 47, no. 22, pp. 6368–6370, May 2011.
- [140] N. Gao, W. Zhou, X. Jiang, G. Hong, T.-M. Fu, and C. M. Lieber, “General strategy for biodetection in high ionic strength solutions using transistor-based nanoelectronic sensors,” *Nano Lett.*, vol. 15, no. 3, pp. 2143–2148, 2015.
- [141] H.-K. Chang *et al.*, “Rapid, label-free, electrical whole blood bioassay based on nanobiosensor systems,” *ACS Nano*, vol. 5, no. 12, pp. 9883–9891, Nov. 2011.
- [142] A. Poghossian, S. Ingebrandt, A. Offenhäusser, and M. J. Schöning, “Field-effect devices for detecting cellular signals,” *Seminars Cell Develop. Biol.*, vol. 20, no. 1, pp. 41–48, Feb. 2009.
- [143] B.-R. Li, C.-C. Chen, U. R. Kumar, and Y.-T. Chen, “Advances in nanowire transistors for biological analysis and cellular investigation,” *Analyst*, vol. 139, no. 7, pp. 1589–1608, Dec. 2014.
- [144] B. Tian, T. Cohen-Karni, Q. Qing, X. Duan, P. Xie, and C. M. Lieber, “Three-dimensional, flexible nanoscale field-effect transistors as localized bioprobes,” *Science*, vol. 329, no. 5993, pp. 830–834, Aug. 2010.
- [145] L. Xu, Z. Jiang, Q. Qing, L. Mai, Q. Zhang, and C. M. Lieber, “Design and synthesis of diverse functional kinked nanowire structures for nanoelectronic bioprobes,” *Nano Lett.*, vol. 13, no. 2, pp. 746–751, 2013.
- [146] T.-S. Pui, A. Agarwal, F. Ye, Y. Huang, and P. Chen, “Nanoelectronic detection of triggered secretion of pro-inflammatory cytokines using CMOS compatible silicon nanowires,” *Biosensors Bioelectron.*, vol. 26, no. 5, pp. 2746–2750, Oct. 2011.
- [147] N. Jokilaakso *et al.*, “Ultra-localized single cell electroporation using silicon nanowires,” *Lab Chip*, vol. 13, no. 3, pp. 336–339, 2013.



**LUYE MU** received the B.A.Sc. degree in nanotechnology engineering from the University of Waterloo, Canada, in 2011. She is currently pursuing the Ph.D. degree with the Department of Electrical Engineering, Yale University. Her research interests include nano-FET biosensors and microfluidic sample manipulation.



**YE CHANG** received the B.S. degree from Tianjin University, Tianjin, China, in 2013, where he is currently pursuing the Ph.D. degree. His research interests include film bulk acoustic resonator chemical sensors and chemical functionalization of micro/nanodevices.



**SONYA D. SAWTELLE** received the B.S. degree in physics from Indiana University. She is currently pursuing the Ph.D. degree with the Department of Applied Physics, Yale University. Her research interests include protein sensing with CMOS compatible FET sensors and single molecule charge transport in small organic molecules and biomacromolecules.



**MATHIAS WIPF** received the B.S. and M.S. degrees in nanosciences and the Ph.D. degree in experimental physics from the University of Basel, Switzerland, in 2008, 2010, and 2014, respectively. He is currently a Post-Doctoral Researcher with the Department of Electrical Engineering, Yale University. His research is focused on silicon-based nanowire sensors for biosensing applications.



**XUEXIN DUAN** received the B.S. and M.S. degrees from Nankai University, Tianjin, China, in 2001 and 2004, respectively, and the Ph.D. degree from the University of Twente, Enschede, The Netherlands, in 2010. He worked for one year with the Max-Planck Institute for Polymer Research, Mainz, Germany. From 2010 to 2013, he was with Yale University as a Post-Doctoral Researcher. He is currently a Professor with Tianjin University. His research

focuses on micro/nanofabricated devices and their applications in chemical or biomolecular sensing.



**MARK A. REED** (SM'97) received the B.S. (Hons.) and M.S. degrees in physics and the Ph.D. degree in solid-state physics from Syracuse University, Syracuse, NY, in 1977, 1979, and 1983, respectively. He was with Texas Instruments, Ultrasmall Electronics Branch, as a member of the Technical Staff, where he cofounded the Nanoelectronics Research Program. In 1988, he was elected as a Senior Member of the Technical Staff. In 1990, he joined as a Faculty Member

with Yale University, New Haven, CT, where he holds a joint appointment as a Professor with the Department of Electrical Engineering and the Department of Applied Physics. He is the Harold Hodgkinson Chair of Engineering and Applied Science and the Associate Director of the Yale Institute for Nanoscience and Quantum Engineering. He has authored over 175 professional publications and six books, has given 20 plenary and over 280 invited talks, and holds 25 U.S. and foreign patents. His research activities include the investigation of electronic transport in nanoscale and mesoscopic systems, heterojunction materials and devices, molecular-scale electronic transport, plasmonic transport in nanostructures, and chem/bionanosensors. He is a fellow of the American Physical Society and a member of the Connecticut Academy of Science and Engineering. His awards include the Kilby Young Innovator Award (1994), the Fujitsu ISCS Quantum Device Award (2001), the Yale Science and Engineering Association Award for Advancement of Basic and Applied Science (2002), and the IEEE Pioneer Award in Nanotechnology (2007). He is an Editor of the IEEE TRANSACTIONS ON ELECTRON DEVICES.

• • •